

INJECTION, EXTRACTION AND MATCHING

M. Ferrario

INFN-LNF

Abstract

In this lecture we introduce from basic principles the main concepts of beam focusing and transport in modern accelerators using the beam envelope equation as a convenient mathematical tool. Matching conditions suitable to preserve the beam quality are derived from the model for significant beam dynamics regimes. An extension of the model to the plasma accelerator case is introduced. The understanding of similarities and differences with respect to traditional accelerators are also emphasized.

1. INTRODUCTION

Light sources based on high gain free electron lasers or future high energy linear colliders require the production, acceleration and transport up to the interaction point of low divergence, high charge density electron bunches [1]. Many effects contribute in general to the degradation of the final beam quality, including chromatic effects, wake fields, emission of coherent radiation, accelerator misalignments. Space charge effects and mismatch with the focusing and accelerating devices typically contribute to emittance degradation of high charge density beams [2], hence the control of beam transport and acceleration is the leading edge for high quality beam production.

In particular further development of plasma based accelerators requires careful phase space matching between plasma acceleration stages and between plasma stages and traditional accelerator components. It represents a very critical issue and a fundamental challenge for high quality beam production and its applications. Without proper matching significant emittance growth may occur when the beam is propagating through different stages and components due to the large differences of transverse focusing strength. This unwanted effect is even more serious in the presence of finite energy spread.

In this lecture we introduce from basic principles the main concepts of beam focusing and transport in modern accelerators using the beam envelope equation as a convenient mathematical tool. Matching conditions suitable to preserve the beam quality are derived from the model for significant beam dynamics regimes. An extension of the model to the plasma accelerator case is introduced. The understanding of similarities and differences with respect to traditional accelerators are also emphasized. A more detailed discussion of the previous topics can be found in the many classical textbooks on this subject as the one listed in references [3,4,5,6].

2. – Laminar and non-laminar beams

An ideal high charge particle beam has orbits that flow in layers that never intersect, as occurs in a laminar fluid. Such a beam is often called laminar beam. More precisely a laminar beam satisfies the following two conditions [6]:

1. All particles at a given position have identical transverse velocities. On the contrary the orbits of two particles that start at the same position could separate and later cross each other.
2. Assuming the beam propagates along the z axis, the magnitudes of the slopes of the trajectories in the transverse directions x and y , given by $x'(z) = \frac{dx}{dz}$ and $y'(z) = \frac{dy}{dz}$, are linearly proportional to the displacement from the axis z of beam propagation.

Trajectories of interest in beam physics are always confined inside of small, near-axis regions, and the transverse momentum is much smaller than the longitudinal momentum, $p_{x,y} \ll p_z \approx p$. As a consequence is convenient in most cases to use the small angle, or *paraxial*, approximation, which allows us to write the useful approximate expressions,

$$x' = \frac{p_x}{p_z} \approx \frac{p_x}{p} \quad \text{and} \quad y' = \frac{p_y}{p_z} \approx \frac{p_y}{p}.$$

To help understanding the features and the advantages of a laminar beam propagation, the following figures compare the typical behavior of a laminar and of a non-laminar (or thermal) beam.

Figure 1 illustrates an example of orbits evolution of a laminar mono-energetic beam with half width x_0 along a simple beam line with an ideal focusing element (solenoid, magnetic quadrupoles or electrostatic transverse fields are usually adopted to this end), represented by a thin lens located at the longitudinal coordinate $z=0$. In an ideal lens focusing (defocusing) forces are linearly proportional to the displacement from the symmetry axis z so that the lens maintains the laminar flow of the beam.

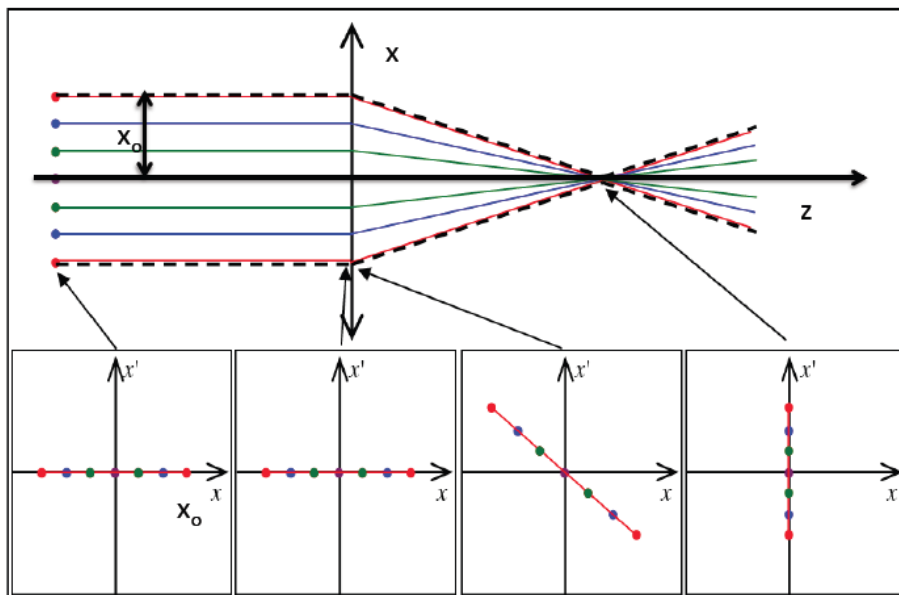


Fig. 1 Particle trajectories and phase space evolution of a laminar beam [21].

The beam of fig. 1 starts propagating completely parallel to the symmetry axis z ; in this particular case particles have all zero transverse velocity. There are no orbits that cross

each other in such a beam. Neglecting collisions and inner forces, like Coulomb forces, such a parallel beam could propagate an infinite distance with no change in its transverse width. When the beam crosses the ideal lens it is transformed in a converging laminar beam. Because the transverse velocities after the linear lens are proportional to the displacement off axis, particle orbits define similar triangles that converge to a single point. After passing through the singularity at the focal point, the particles follow diverging orbits. We can always transform a diverging (or converging) beam to a parallel beam by using a lens of the proper focal length, as can be seen reversing the propagation axis of fig. 1.

The small boxes in the lower part of figure depict the particle distributions in the trace space (x, x') , equivalent to the canonical phase space $(x, p_x \approx x'p)$ when p is constant i.e. without beam acceleration. The phase space area occupied by a ideal laminar beam is a straight segment of zero thickness. As can be easily verified the condition that the particle distribution has zero thickness proceeds from condition 1; the segment straightness is a consequence of condition 2. The distribution of a laminar beam propagating through a transport system with ideal linear focusing elements is thus a straight segment with variable slope.

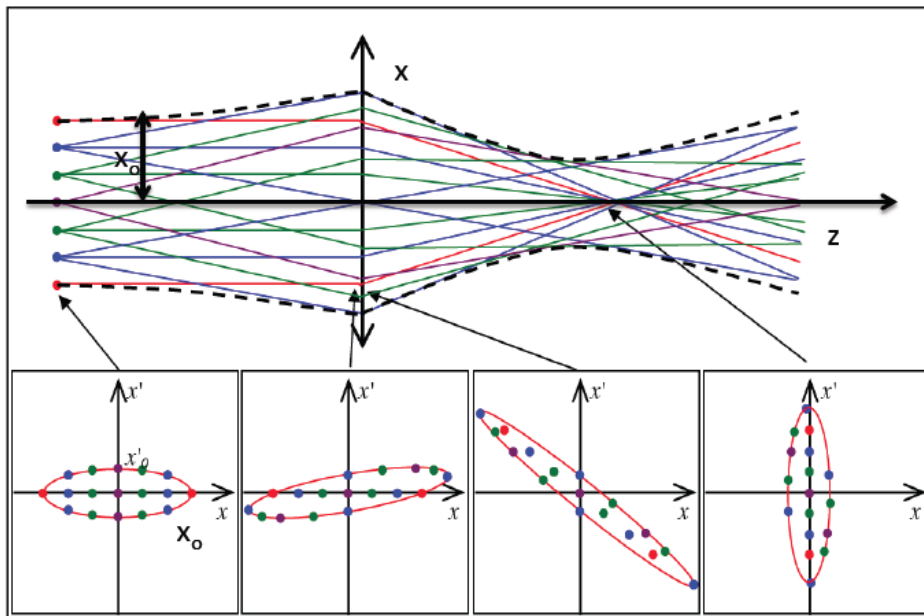


Fig. 2 Particle trajectories and phase space evolution of a non-laminar beam [21].

Particles in a non-laminar beam have a random distribution of transverse velocities at the same location and a spread in directions, as shown in fig. 2. Because of the disorder of a non-laminar beam, it is impossible to focus all particles from a location in the beam toward a common point. Lenses can influence only the average motion of particles. Focal spot limitations are a major concern for a wide variety of applications, from electron microscopy to free electron lasers and linear colliders. The phase space plot of a non-laminar beam is not anymore a straight line: the beam, as shown in the lower boxes of fig. 2, occupies a wider area of the phase space.

3. - The emittance concept

The phase space surface A occupied by a beam is a convenient figure of merit to designate the quality of a beam. This quantity is the emittance ϵ_x and is represented by an ellipse that contains the whole particle distribution in the phase space (x, x') , such that $A = \pi\epsilon_x$. An analogous definition holds for the (y, y') and (z, z') planes. The original choice of an elliptical shape comes from the fact that when linear focusing forces are applied to a beam, the trajectory of each particle in phase space lies on an ellipse, which may be called the trajectory ellipse. Being the area of the phase space, the emittance is measured in [mm-mrad] or more often in [μm].

The ellipse equation is written as:

$$(1) \quad \gamma_x x^2 + 2\alpha_x x x' + \beta_x x'^2 = \epsilon_x$$

where x and x' are the particle coordinates in the phase space and the coefficients $\alpha_x(z), \beta_x(z), \gamma_x(z)$ are called Twiss parameters which are related by the geometrical condition:

$$(2) \quad \beta_x \gamma_x - \alpha_x^2 = 1$$

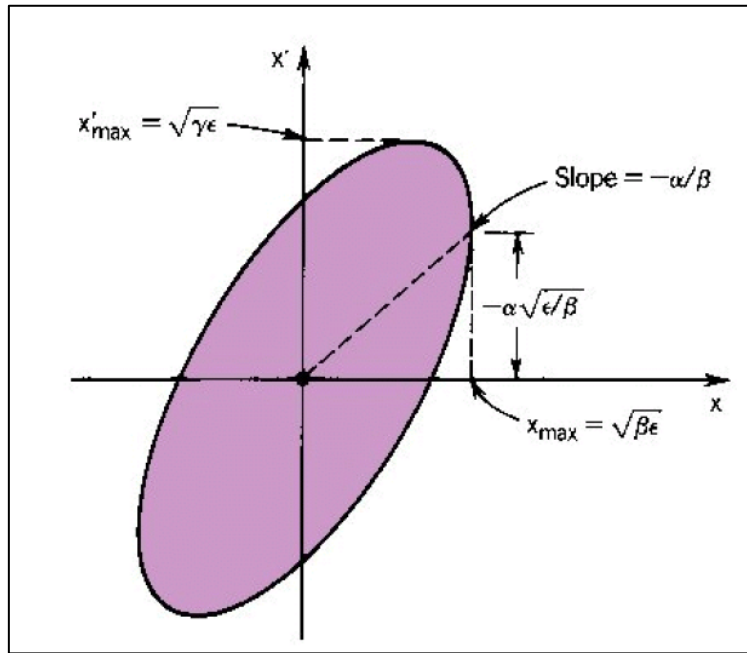


Fig. 3 Phase space distribution in a skewed elliptical boundary showing relationship of Twiss parameters to the ellipse geometry [6].

As shown in fig. 3 the beam envelope boundary X_{\max} , its derivative $(X_{\max})'$ and the maximum beam divergency X'_{\max} , i.e. the projection on the axis x and x' of the ellipse edges, can be expressed as a function of the ellipse parameters:

$$(3) \quad \begin{cases} X_{\max} = \sqrt{\beta_x \varepsilon_x} \\ (X_{\max})' = -\alpha \sqrt{\frac{\varepsilon}{\beta}} \\ X'_{\max} = \sqrt{\gamma_x \varepsilon_x} \end{cases}$$

According to Liouville theorem the 6D (x, p_x, y, p_y, z, p_z) phase space volume occupied by a beam is constant, provided that there are no dissipative forces, no particles lost or created, and no Coulomb scattering among particles. Moreover if the forces in the three orthogonal directions are uncoupled, Liouville theorem holds also for each reduced phase space $(x, p_x), (y, p_y), (z, p_z)$ surfaces and hence also emittance remains constant in each plane [3]. Although the net phase space surface occupied by a beam is constant, nonlinear field components can stretch and distort the particle distribution in the phase space and the beam lose its laminar behavior. A realistic phase space distribution is often well different by a regular ellipse, as shown in the fig. 4.

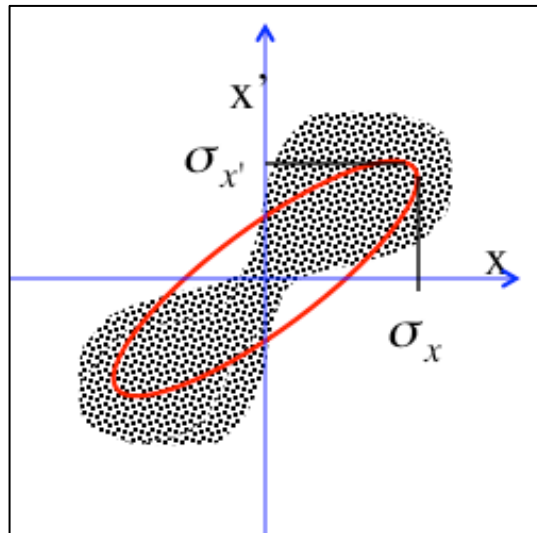


Fig. 4 – Typical evolution of phase space distribution (black dots) under the effects of non linear forces with superimposed the equivalent ellipse (red line).

We introduce, therefore, a definition of emittance that measures the beam quality rather than the phase space area. It is often more convenient to associate to a generic distribution function $f(x, x', z)$ in the phase space a statistical definition of emittance, the so called *rms emittance*:

$$(4) \quad \gamma_x x^2 + 2\alpha_x x x' + \beta_x x'^2 = \varepsilon_{x,rms}$$

such that the ellipse projections on the x and x' axes are equal to the rms values of the distribution, implying the following conditions:

$$(5) \quad \begin{cases} \sigma_x = \sqrt{\beta_x \varepsilon_{x,rms}} \\ \sigma_{x'} = \sqrt{\gamma_x \varepsilon_{x,rms}} \end{cases}$$

where

$$(6) \quad \begin{cases} \sigma_x^2(z) = \langle x^2 \rangle = \int_{-\infty}^{+\infty} \int_{-\infty}^{+\infty} x^2 f(x, x', z) dx dx' \\ \sigma_{x'}^2(z) = \langle x'^2 \rangle = \int_{-\infty}^{+\infty} \int_{-\infty}^{+\infty} x'^2 f(x, x', z) dx dx' \end{cases}$$

are the second moments of the distribution function $f(x, x', z)$. Another important quantity that accounts for the degree of (x, x') correlations is defined as:

$$(7) \quad \sigma_{xx'}(z) = \langle xx' \rangle = \int_{-\infty}^{+\infty} \int_{-\infty}^{+\infty} xx' f(x, x', z) dx dx'$$

From relations (3) it holds also $\sigma_{x'} = \frac{\sigma_{xx'}}{\sigma_x} = -\alpha_x \sqrt{\frac{\varepsilon_{x,rms}}{\beta_x}}$, see also eq. (16), which allows us to link the correlation moment (7) to the Twiss parameter as:

$$(8) \quad \sigma_{xx'} = -\alpha_x \varepsilon_{x,rms}$$

One can easily see from relations (3) and (5) that holds also: $\alpha_x = -\frac{1}{2} \frac{d\beta_x}{dz}$.

By substituting the Twiss parameter defined by (5) and (8) into the condition (2) we obtain [5]:

$$(9) \quad \frac{\sigma_{x'}^2}{\varepsilon_{x,rms}} \frac{\sigma_x^2}{\varepsilon_{x,rms}} - \left(\frac{\sigma_{xx'}}{\varepsilon_{x,rms}} \right)^2 = 1$$

Reordering the terms in (8) we end up with the definition of *rms emittance* in terms of the second moments of the distribution:

$$(10) \quad \varepsilon_{rms} = \sqrt{\sigma_x^2 \sigma_{x'}^2 - \sigma_{xx'}^2} = \sqrt{\left(\langle x^2 \rangle \langle x'^2 \rangle - \langle xx' \rangle^2 \right)}$$

where we omit, from now on, the subscribed x in the emittance notation: $\varepsilon_{rms} = \varepsilon_{x,rms}$. Rms emittance tells us some important information about phase space distributions under the effect of linear or non-linear forces acting on the beam. Consider for example an idealized particle distribution in phase space that lies on some segment that passes through the origin as illustrated in fig. 5.

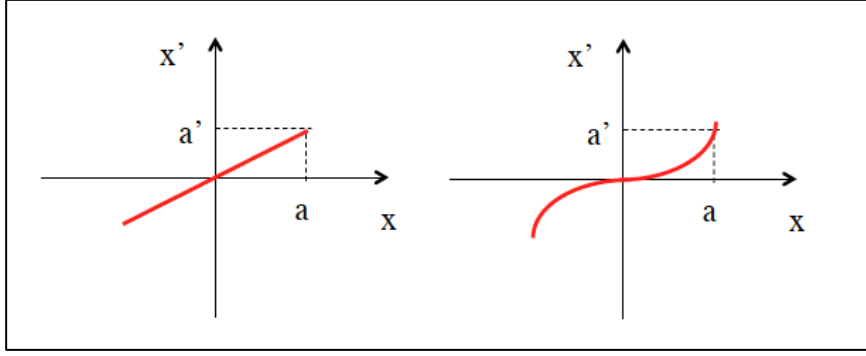


Fig. 5 - Phase space distributions under the effect of linear (left) or non-linear (right) forces acting on the beam

Assuming a generic correlation of the type $x' = Cx^n$ and computing the rms emittance according to (10) we have:

$$(11) \quad \varepsilon_{rms}^2 = C \sqrt{\langle x^2 \rangle \langle x^{2n} \rangle - \langle x^{n+1} \rangle^2} \quad \begin{cases} n = 1 & \Rightarrow \varepsilon_{rms} = 0 \\ n > 1 & \Rightarrow \varepsilon_{rms} \neq 0 \end{cases}$$

When $n=1$ the line is straight and the rms emittance is $\varepsilon_{rms} = 0$. When $n>1$ the relationship is nonlinear, the line in phase space is curved, and the rms emittance is in general not zero. Both distributions have zero area. Therefore, we conclude that even when the phase-space area is zero, if the distribution lies on a curved line its rms emittance is not zero. The rms emittance depends not only on the area occupied by the beam in phase space but also on distortions produced by non-linear forces.

If the beam is subject to acceleration it is more convenient to use the rms normalized emittance, for which the transverse momentum $p_x = p_z x' = m_o c \beta \gamma x'$ is used instead of the divergence:

$$(12) \quad \varepsilon_{n,rms} = \frac{1}{m_o c} \sqrt{\sigma_x^2 \sigma_{p_x}^2 - \sigma_{x p_x}^2} = \frac{1}{m_o c} \sqrt{\langle x^2 \rangle \langle p_x^2 \rangle - \langle x p_x \rangle^2} = \sqrt{\langle x^2 \rangle \langle (\beta \gamma x')^2 \rangle - \langle x \beta \gamma x' \rangle^2}$$

The reason for introducing a normalized emittance is that the divergences of the particles $x' = p_x / p$ are reduced during acceleration as p increases. Thus acceleration reduces the un-normalized emittance but does not affect the normalized emittance. Assuming small energy spread within the beam, the normalized and un-normalized emittances can be related by the approximated relation: $\langle \beta \gamma \rangle \varepsilon_{rms}$. This approximation that is often used in conventional accelerators may be strongly misleading when adopted to describe beams with significant energy spread, as the one at present produced by plasma accelerators. A more careful analysis is reported hereafter following [17].

When the correlations between the energy and transverse positions are negligible (as in a drift without collective effects), eq. (12) can be written as:

$$(13) \quad \varepsilon_{n,rms}^2 = \langle \beta^2 \gamma^2 \rangle \langle x^2 \rangle \langle x'^2 \rangle - \langle \beta \gamma \rangle^2 \langle x x' \rangle^2$$

Considering now the definition of relative energy spread $\sigma_\gamma^2 = \frac{\langle \beta^2 \gamma^2 \rangle - \langle \beta \gamma \rangle^2}{\langle \beta \gamma \rangle^2}$ which can be inserted in eq. (13) to give:

$$(14) \quad \varepsilon_{n,rms}^2 = \langle \beta^2 \gamma^2 \rangle \sigma_\gamma^2 \langle x^2 \rangle \langle x'^2 \rangle + \langle \beta \gamma \rangle^2 \left(\langle x^2 \rangle \langle x'^2 \rangle - \langle x x' \rangle^2 \right)$$

Assuming relativistic electrons ($\beta = 1$) we get

$$(15) \quad \varepsilon_{n,rms}^2 = \langle \gamma^2 \rangle \left(\sigma_\gamma^2 \sigma_x^2 \sigma_{x'}^2 + \varepsilon_{rms}^2 \right)$$

If the first term in the parentheses is negligible, we find the conventional approximation of normalized emittance, as $\langle \gamma \rangle \varepsilon_{rms}$. For a conventional accelerator this might generally be the case. Considering for example beam parameters as for the SPARC_LAB photoinjector [18], at 5 MeV the ratio between the first and the second term is $\sim 10^{-3}$ while at 150 MeV it is $\sim 10^{-5}$. On the other hand using typical beam parameters at the plasma-vacuum interface the first term is of the same order of magnitude as for conventional accelerators at low energies; however, due to the rapid increase of the bunch size outside the plasma ($\sigma_{x'} \sim \text{mrad}$) and the large energy spread ($\sigma_\gamma > 1\%$), it becomes predominant compared to the second term after few mm long drift. *Therefore the use of approximated formulas when measuring the normalized emittance of plasma accelerated particle beams is very inappropriate [19].*

4. – The rms envelope equation

We are now interested to follow the evolution of the particle distribution during beam transport and acceleration. One can take profit of the first collective variable defined in eq. (6), the second moment of the distribution termed rms beam envelope, to derive a differential equation suitable to describe the rms beam envelope dynamics [7]. To this end lets compute the first and second derivative of σ_x [4]:

$$(16) \quad \begin{aligned} \frac{d\sigma_x}{dz} &= \frac{d}{dz} \sqrt{\langle x^2 \rangle} = \frac{1}{2\sigma_x} \frac{d}{dz} \langle x^2 \rangle = \frac{1}{2\sigma_x} 2 \langle x x' \rangle = \frac{\sigma_{xx'}}{\sigma_x} \\ \frac{d^2\sigma_x}{dz^2} &= \frac{d}{dz} \frac{\sigma_{xx'}}{\sigma_x} = \frac{1}{\sigma_x} \frac{d\sigma_{xx'}}{dz} - \frac{\sigma_{xx'}^2}{\sigma_x^3} = \frac{1}{\sigma_x} \left(\langle x'^2 \rangle + \langle x x'' \rangle \right) - \frac{\sigma_{xx'}^2}{\sigma_x^3} = \frac{\sigma_{x'}^2 + \langle x x'' \rangle}{\sigma_x} - \frac{\sigma_{xx'}^2}{\sigma_x^3} \end{aligned}$$

Rearranging the second derivative (16) we obtain a second order non linear differential equation for the beam envelope evolution:

$$(17) \quad \sigma_x'' = \frac{\sigma_x^2 \sigma_{x'}^2 - \sigma_{xx'}^2}{\sigma_x^3} + \frac{\langle x x'' \rangle}{\sigma_x}$$

or in a more convenient form using the rms emittance definition (10):

$$(18) \quad \sigma_x'' - \frac{1}{\sigma_x} \langle xx'' \rangle = \frac{\varepsilon_{r.m.s.}^2}{\sigma_x^3}$$

In the equation (18) the emittance term can be interpreted physically as an outward pressure on the beam envelope produced by the rms spread in trajectory angle, which is parameterized by the rms emittance.

Lets now consider for example the simple case with $\langle xx'' \rangle = 0$, describing a beam drifting in the free space. The envelope equation reduces to:

$$(19) \quad \sigma_x^3 \sigma_x'' = \varepsilon_{rms}^2$$

With initial conditions σ_o, σ_o' at z_o , depending on the upstream transport channel, equation (19) has a hyperbolic solution:

$$(20) \quad \sigma(z) = \sqrt{\left(\sigma_o + \sigma_o'(z - z_o)\right)^2 + \frac{\varepsilon_{rms}^2}{\sigma_o^2} (z - z_o)^2}$$

Considering the case of a beam at waist ($\langle xx' \rangle = 0$) with $\sigma_o' = 0$, using definition (5) the solution (20) is often written in terms of the β function as:

$$(21) \quad \sigma(z) = \sigma_o \sqrt{1 + \left(\frac{z - z_o}{\beta_w}\right)^2}$$

This relation indicates that without any external focusing element the beam envelope increases from the beam waist by a factor $\sqrt{2}$ with a characteristic length $\beta_w = \frac{\sigma_o^2}{\varepsilon_{rms}}$ as shown if fig 6.

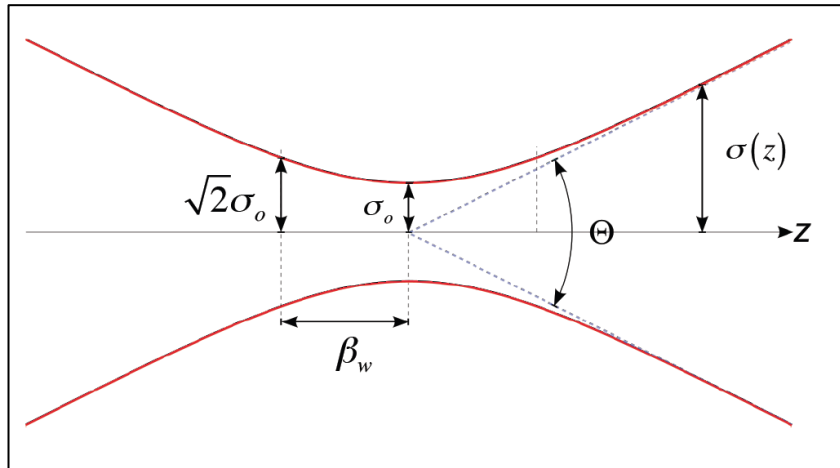


Fig. 6 – Schematic representation of the beam envelope behavior near the beam waist.

At waist holds also the relation $\varepsilon_{rms}^2 = \sigma_{o,x}^2 \sigma_{o,x'}$ that can be inserted in eq. (20) to get $\sigma_x^2(z) = \sigma_{o,x'}^2 (z - z_o)^2$. Under this condition eq (15) can be written as follows:

$$\varepsilon_{n,rms}^2(z) = \langle \gamma^2 \rangle \left(\sigma_\gamma^2 \sigma_x^4 (z - z_o)^2 + \varepsilon_{rms}^2 \right)$$

showing that beams with large energy spread an divergence undergo a significant normalized

emittance growth even in a drift of length $(z-z_0)$ [17,20].

Notice also that the solution (21) is exactly analogous to that of a Gaussian light beam for which the beam width $w = 2\sigma_{ph}$ increases away from its minimum value at the waist w_0 with characteristic length $Z_R = \frac{\pi w_0^2}{\lambda}$ (Rayleigh length) [4]. This analogy suggests that we can identify an effective emittance of a photon beam as $\varepsilon_{ph} = \frac{\lambda}{4\pi}$.

For an effective transport of a beam with finite emittance is mandatory to make use of some external force providing beam confinement in the transport or accelerating line. The term $\langle xx'' \rangle$ accounts for external forces when we know x'' given by the single particle equation of motion:

$$(22) \quad \frac{dp_x}{dt} = F_x$$

Under the paraxial approximation $p_x \ll p = \beta\gamma mc$ the transverse momentum p_x can be written as $p_x = px' = \beta\gamma m_0 c x'$, so that:

$$(23) \quad \frac{dp_x}{dt} = \frac{d}{dt}(px') = \beta c \frac{d}{dz}(px') = F_x$$

and the transverse acceleration results to be:

$$(24) \quad x'' = -\frac{p'}{p}x' + \frac{F_x}{\beta cp}$$

It follows that:

$$(25) \quad \langle xx'' \rangle = -\frac{p'}{p}\langle xx' \rangle + \frac{\langle xF_x \rangle}{\beta cp} = -\frac{p'}{p}\sigma_{xx'} + \frac{\langle xF_x \rangle}{\beta cp}$$

Inserting eq. (25) in eq. (18) and recalling eq. (16) $\sigma'_x = \frac{\sigma_{xx'}}{\sigma_x}$, the complete rms envelope equation results to be:

$$(26) \quad \sigma_x'' + \frac{p'}{p}\sigma_x' - \frac{1}{\sigma_x} \frac{\langle xF_x \rangle}{\beta cp} = \frac{\varepsilon_{n,rms}^2}{\gamma^2 \sigma_x^3}$$

where we have included the normalized emittance $\varepsilon_{n,rms} = \gamma\varepsilon_{rms}$. Notice that the effect of longitudinal accelerations appears in the rms envelope equation as an oscillation damping term, called “adiabatic damping”, proportional to $\frac{p'}{p}$. The term $\langle xF_x \rangle$ represents the moment of any external transverse force acting on the beam, as the one produced by a focusing magnetic channel.

5. – External forces

Lets now consider the case of external linear force acting on the beam in the form $F_x = \mp kx$. It can be focusing or defocussing according to the sign. The moment of the force results to be:

$$(27) \quad \langle xF_x \rangle = \mp k \langle x^2 \rangle = \mp k \sigma_x^2$$

and the envelope equation becomes:

$$(28) \quad \sigma_x'' + \frac{\gamma'}{\gamma} \sigma_x' \mp k_{ext}^2 \sigma_x = \frac{\epsilon_{n,rms}^2}{\gamma^2 \sigma_x^3}$$

where we have explicitly used the momentum definition $p = \gamma mc$ for a relativistic particle with $\beta \approx 1$ and defined the wavenumber $k_{ext}^2 = \frac{k}{\gamma m_o c^2}$.

Typical focusing elements are quadrupoles and solenoids [3]. The magnetic quadrupole field in Cartesian coordinates is given by:

$$(29) \quad \begin{cases} B_x = B_o \frac{y}{d} = B_o' y \\ B_y = B_o \frac{x}{d} = B_o' x \end{cases}$$

where d is the pole distance and B_o' the field gradient. The force acting on the beam is $\vec{F}_\perp = qv_z B_o' (y\hat{j} - x\hat{i})$ that, when B_o is positive, is focusing in the x direction and defocusing in y. The focusing strength is $k_{quad} = \frac{qB_o'}{\gamma m_o c} = k_{ext}^2$.

In a solenoid the focusing strength is given by: $k_{sol} = \left(\frac{qB_o}{2\gamma m_o c} \right)^2 = k_{ext}^2$. Notice that the solenoid is always focusing in both directions, an important properties when the cylindrical symmetry of the beam must be preserved. On the other hand being a second order quantity in γ it is more effective at low energy.

It is interesting to consider the case of a uniform focusing channel without acceleration described by the rms envelope equation:

$$(30) \quad \sigma_x'' + k_{ext}^2 \sigma_x = \frac{\epsilon_{rms}^2}{\sigma_x^3}$$

By substituting $\sigma_x = \sqrt{\beta_x \epsilon_{rms}}$ in (30) one obtains an equation for the ‘‘betatron function’’ $\beta_x(z)$ that is independent on the emittance term:

$$(31) \quad \beta_x'' + 2k_{ext}^2 \beta_x = \frac{2}{\beta_x} + \frac{\beta_x'^2}{2\beta_x}$$

Equation (31) containing only the transport channel focusing strength and being independent on the beam parameters, suggests that the meaning of the betatron function is to describe the

transport line characteristic by itself. The betatron function reflects exterior forces from focusing magnets and is highly dependent on the particular arrangement of quadrupole magnets. The equilibrium, or matched, solution of eq. (31) is given by $\beta_{eq} = \frac{1}{k_{ext}} = \frac{\lambda_\beta}{2\pi}$ as one can easily verify. This result shows that the matched β_x function is simply the inverse of the focusing wave number, or equivalently is proportional to the “betatron wavelength” λ_β

6. - Space charge forces

Another important force acting on the beam is the one produced by the beam itself due to the internal Coulomb forces. The net effect of the Coulomb interaction in a multi-particle system can be classified into two regimes [3]:

- *Collisional regime*, dominated by binary collisions caused by close particle encounters

- *Collective regime or space charge regime*, dominated by the self-field produced by the particle’s distribution that varies appreciably only over large distances compare to the average separation of the particles.

A measure for the relative importance of collisional versus collective effects in a beam with particle density n is the relativistic *Debye length*:

$$(32) \quad \lambda_D = \sqrt{\frac{\epsilon_0 \gamma^2 k_B T_b}{e^2 n}}$$

where the transverse beam temperature T_b is defined as $k_B T_b = \gamma m_o \langle v_\perp^2 \rangle$, and k_B is the Boltzmann constant. As long as the Debye length remains small compared to the particle bunch transverse size the beam is in the space charge dominated regime and is not sensitive to binary collisions. Smooth functions for the charge and field distributions can be used in this case and the space charge force can be treated like an external applied force. The space-charge field can be separated into linear and nonlinear terms as a function of displacement from the beam axis. The linear space-charge term defocuses the beam and leads to an increase in beam size. The nonlinear space-charge terms increase also the rms emittance by distorting the phase-space distribution. Under the paraxial approximation of particle motion we can consider the linear component only. We shall see in the next paragraph that also the linear component of the space charge field can induce emittance growth when correlation along the bunch are taken in to account.

For a bunched beam of uniform charge distribution in a cylinder of radius R and length L , carrying a current \hat{I} and moving with longitudinal velocity $v_z = \beta c$, the linear component of the longitudinal and transverse space charge field are approximately given by [8]:

$$(33) \quad E_z(\xi) = \frac{\hat{I}L}{2\pi\epsilon_0 R^2 \beta c} h(\xi)$$

$$(34) \quad E_r(r, \xi) = \frac{\hat{I}r}{2\pi\epsilon_0 R^2 \beta c} g(\xi)$$

The field form factor is described by the functions:

$$(35) \quad h(\xi) = \left[\sqrt{A + (1 - \xi)^2} - \sqrt{A + \xi^2} + (2\xi - 1) \right]$$

$$(36) \quad g(\xi) = \frac{(1 - \xi)}{2\sqrt{A^2 + (1 - \xi)^2}} + \frac{\xi}{2\sqrt{A^2 + \xi^2}}$$

where $\xi = \frac{z}{L}$ is the normalized longitudinal coordinate along the bunch and $A = \frac{R}{\gamma L}$ is the beam aspect ratio. The field form factors account for the longitudinal variation of the fields along the bunch. As γ increases $g(\xi) \rightarrow 1$ and $h(\xi) \rightarrow 0$ thus showing that space charge fields mainly affect transverse beam dynamics. It shows also that an energy increase corresponds to a bunch lengthening in the moving frame $L' = \gamma L$ leading to a vanishing longitudinal field component, as in the case of a continuous beam in the laboratory frame.

To evaluate the force acting on the beam one must account also for the azimuthal magnetic field associated with the beam current, that in cylindrical symmetry is given by

$B_\theta = \frac{\beta}{c} E_r$. Thus the Lorentz force acting on each single particle is given by:

$$(37) \quad F_r = e(E_r - \beta c B_\theta) = e(1 - \beta^2)E_r = \frac{eE_r}{\gamma^2}$$

The attractive magnetic force, which becomes significant at high velocities, tends to compensate for the repulsive electric force. Therefore space charge defocusing is primarily a non-relativistic effect and decreases as γ^{-2} .

In order to include space charge forces in the envelope equation lets start writing the space charge forces produced by the previous fields in Cartesian coordinates:

$$(38) \quad F_x = \frac{e\hat{I}x}{2\pi\gamma^2\epsilon_0\sigma_x^2\beta c} g(\xi)$$

Then computing the moment of the force we need:

$$(39) \quad x'' = \frac{F_x}{\beta c p} = \frac{eIx}{2\pi\epsilon_0\gamma^3 m_0\beta^3 c^3\sigma_x^2} g(\xi) = \frac{k_{sc}(\xi)}{(\beta\gamma)^3\sigma_x^2} x$$

where we have introduced the generalized beam perveance

$$(40) \quad k_{sc}(\xi) = \frac{2\hat{I}}{I_A} g(\xi)$$

normalized to the Alfvén current $I_A = \frac{4\pi\epsilon_0 m_0 c^3}{e} = 17kA$. Notice that in this case the perveance

(40) explicitly depends on the slice coordinate ξ . Now we can calculate the term that enters in the envelope equation for a relativistic beam:

$$(41) \quad \langle xx'' \rangle = \frac{k_{sc}}{\gamma^3 \sigma_x^2} \langle x^2 \rangle = \frac{k_{sc}}{\gamma^3}$$

leading to the complete envelope equation:

$$(42) \quad \sigma_x'' + \frac{\gamma'}{\gamma} \sigma_x' + k_{ext}^2 \sigma_x = \frac{\epsilon_{n,rms}^2}{\gamma^2 \sigma_x^3} + \frac{k_{sc}}{\gamma^3 \sigma_x}$$

From the envelope equation (42) we can identify two regimes of beam propagation: *space charge dominated* and *emittance dominated*. A beam is space charge dominated as long as the space charge collective forces are largely dominant over the emittance pressure. In this regime the linear component of the space charge force produces a quasi-laminar propagation of the beam as one can see by integrating one time eq. (39) under the paraxial ray approximation $x' \ll 1$. A measure of the relative importance of space charge effects versus emittance pressure is given by the *laminarity parameter*, defined as the ratio between the space charge term and the emittance term:

$$(43) \quad \rho = \frac{\hat{I}}{2I_A \gamma} \frac{\sigma^2}{\epsilon_n^2}$$

When ρ greatly exceeds unity, the beam behaves like a laminar flow (all beam particles move on trajectories that do not cross) and transport and acceleration require a careful tuning of focusing and accelerating elements in order to keep laminarity. Correlated emittance growth is typical in this regime which can be conveniently made reversible if proper beam matching conditions are fulfilled, as discussed in the next paragraph. When $\rho < 1$ the beam is emittance dominated (thermal regime) and the space charge effects can be neglected. The transition to thermal regime occurs when $\rho \approx 1$ corresponding to the transition energy

$$(44) \quad \gamma_{tr} = \frac{\hat{I}}{2I_A} \frac{\sigma^2}{\epsilon_n^2}$$

For example a beam with $\hat{I}=100$ A $\epsilon_n=1$ μm and $\sigma=300$ μm is leaving the space charge dominated regime and is entering the thermal regime at the transition energy of 131 MeV. From this example one may conclude that space charge dominated regime is typical of low energy beams. Actually for applications like linac driven Free Electron Lasers peak current exceeding kA are required. Space charge effects may recur if bunch compressors are active at higher energies and a new energy threshold with higher \hat{I} has to be considered.

7. - Correlated emittance oscillations

When longitudinal correlations within the bunch are important, as the one induced by the space charge effects, the beam envelope evolution is generally dependent also on the bunch coordinate ξ . In this case the bunch should be considered as an ensemble of N longitudinal slices of envelope $\sigma_s(z, \xi)$ whose evolution can be computed from N slice

envelope equations equivalent to (42) provided that the bunch parameters refer to each single slice: $\gamma_s, \gamma'_s, k_{sc,s} = k_{sc}g(\xi)$. Correlations within the bunch may cause emittance oscillations that can be evaluated, once an analytical or numerical solution [8] of the slice envelope equation is known, by using the following correlated emittance definition:

$$(45) \quad \varepsilon_{rms,cor} = \sqrt{\langle \sigma_s^2 \rangle \langle \sigma_s'^2 \rangle - \langle \sigma_s \sigma_s' \rangle^2}$$

where the average is performed over the entire slice ensemble. In the simplest case of a 2 slices model the previous definition reduces to:

$$(46) \quad \varepsilon_{rms,cor} = \left| \sigma_1 \sigma_2' - \sigma_2 \sigma_1' \right|$$

that represents a simple and useful formula for an estimation of the emittance scaling [9].

The total normalized rms emittance is the given by the superposition of the correlated and uncorrelated terms as :

$$(47) \quad \varepsilon_{n,rms} = \langle \gamma \rangle \sqrt{\varepsilon_{rms}^2 + \varepsilon_{rms,cor}^2}$$

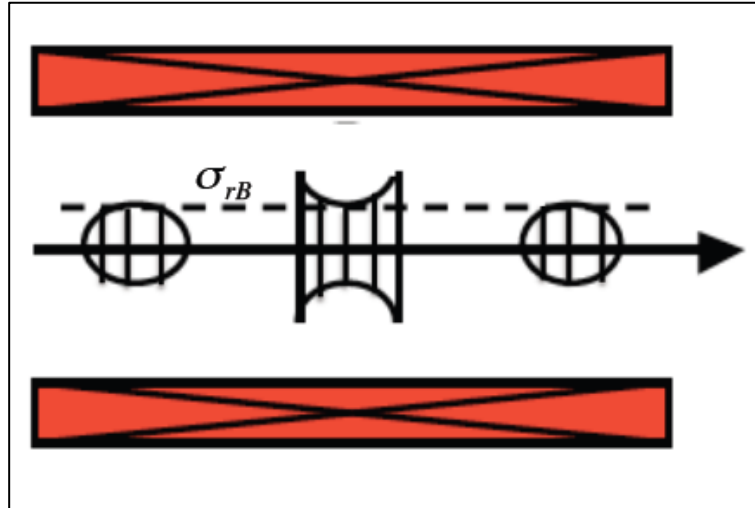


Fig. 7 - Schematic representation of a nearly matched beam in a long solenoid. The dashed line represent the reference slice envelope fully matched to the Brillouin flow condition. The other slice envelopes are oscillating around the equilibrium solution.

An interesting example to consider here, showing the consequences of a non perfect beam matching, is the propagation of a beam in the space charge dominated regime nearly matched to an external focusing channel ($k_{ext} = k_{sol}$), as illustrated in fig. 7. To simplify our computations we can neglect acceleration, as in the case of a simple beam transport line. The envelope equation for each slice, indicated as σ_s , reduces to:

$$(48) \quad \sigma_s'' + k_{ext}^2 \sigma_s = \frac{k_{sc,s}}{\gamma^3 \sigma_s}$$

A stationary solution, called *Brillouin flow*, is given by:

$$(49) \quad \sigma_{s,B} = \frac{1}{k_{ext}^2} \sqrt{\frac{\hat{I}g(\xi)}{2\gamma^3 I_A}}$$

where the local dependence of the current $\hat{I}_s = \hat{I}g(\xi)$ within the bunch has been explicitly indicated. This solution represent the matching conditions for which the external focusing completely balances the internal space charge force. Unfortunately since k_{ext} has a slice independent constant value, the Brillouin matching condition cannot be achieved at the same time for all the bunch slices. Assuming there is a reference slice perfectly matched with an envelope $\sigma_{r,B}$, the matching condition for the other slices can be written as:

$$(50) \quad \sigma_{sB} = \sigma_{rB} + \frac{\sigma_{rB}}{2} \left(\frac{\delta I_s}{\hat{I}} \right)$$

with respect to the reference slice. Considering a small perturbation δ_s from the equilibrium in the form

$$(51) \quad \sigma_s = \sigma_{s,B} + \delta_s$$

and substituting in the equation (48) we can obtain a linearized equation for the slice offset:

$$(52) \quad \delta_s'' + 2k_{ext}^2 \delta_s = 0$$

which has a solution given by:

$$(53) \quad \delta_s = \delta_o \cos(\sqrt{2}k_{ext}z)$$

where $\delta_o = \sigma_{so} - \sigma_{sB}$ is the amplitude of the initial slice mismatch that we assume for convenience the same for all slices. Inserting (53) in (51) we get the perturbed solution:

$$(54) \quad \sigma_s = \sigma_{s,B} + \delta_o \cos(\sqrt{2}k_{ext}z)$$

Equation (54) shows that slice envelopes oscillate altogether around the equilibrium solution with the same frequency for all slices ($\sqrt{2}k_{ext}$, often called plasma frequency) dependent only on the external focusing forces. This solution represents a collective behavior of the bunch similar to the one of the electrons subject to the restoring force of ions in a plasma. Using the two slices model and eq. (54) the emittance evolution (46) results:

$$(55) \quad \varepsilon_{rms,cor} = \frac{1}{4} k_{sol} \sigma_{rB} \left| \frac{\Delta I}{\hat{I}} \delta_o \sin(\sqrt{2}k_{ext}z) \right|$$

where $\Delta I = \hat{I}_1 - \hat{I}_2$. Notice that in this simple case envelope oscillations of the mismatched slices induce correlated emittance oscillations which periodically goes back to zero, showing the reversible nature of the correlated emittance growth. Is, in fact, the coupling between transverse and longitudinal motion induced by the space charge fields that allows reversibility. With a proper tuning of the transport line length or of the focusing field one can compensate for the transverse emittance growth at the expenses of the longitudinal emittance.

At first it may seem surprising that a beam with a single charge species can exhibit plasma oscillations, which are characteristic of plasmas composed of two-charge species. But the effect of the external focusing force can play the role of the other charge species to provide the necessary restoring force that is the cause of such collective oscillations, as shown in fig. 8. The beam can be actually considered as a single component, relativistic, cold plasma.

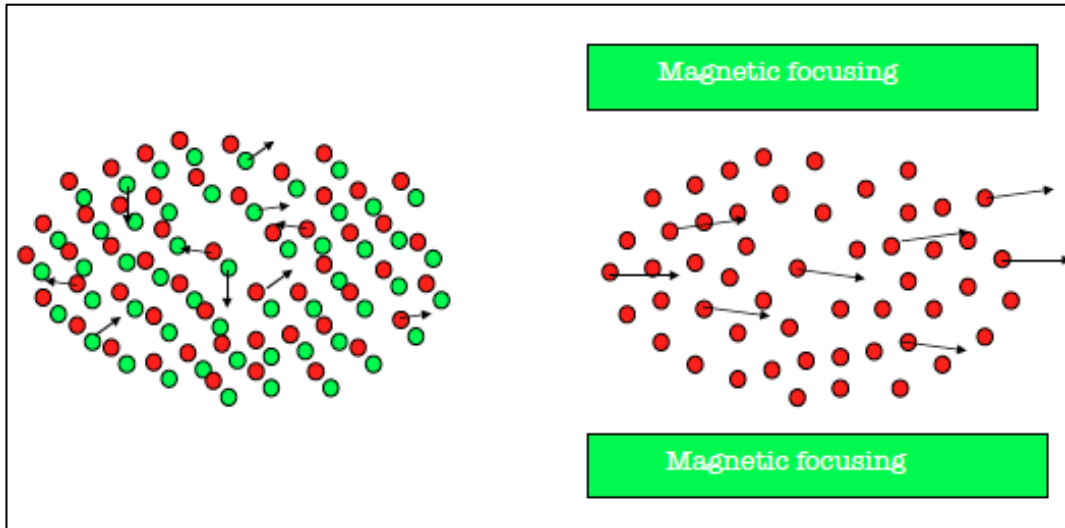


Fig. 8 – The restoring force produced by the ions (green dots) in a plasma may cause electron (red dots) oscillations around the equilibrium distribution. In a similar way the restoring force produced by a magnetic field may cause beam envelope oscillations around the matched envelope equilibrium.

It is important to bear in mind that beams in linacs are also different from plasmas in some important respects [5]. One is that beam transit time through a linac is too short for the beam to reach thermal equilibrium. Also, unlike a plasma, the Debye length of the beam may be larger than or comparable to the beam radius, so shielding effects may be incomplete.

8. - Matching conditions in a Plasma Accelerator

The concepts developed for the beam transport in the previous sections can be now applied to the case of a plasma accelerator [10] giving important information about the critical topic of beam-plasma matching conditions. To this end we introduce a simplified model for the plasma and for the resulting fields acting on the beam in order to be able to write an envelope equation for the accelerated beam.

In this section we are interested in the case of external injection of particles in a plasma wave, in the so called “bubble” regime, that could be excited by a short intense laser pulse [10,11] or by a driving electron beam [12,13] with beam density n_b larger than the plasma density n_o , $n_b > n_o$. A very simplified model for the plasma behind the driving pulse is illustrated in Figure 9. We will consider a spherical uniform ion distribution, as indicated by a dashed circle, with particle density n_o . This model is justified by the fact that in this regime the fields are linear in longitudinal and transverse directions, at least in the region of interest for particle acceleration, as the one produced by a uniform ion distribution within a sphere of radius $R_{sphere} \approx \frac{\lambda_p}{2}$ where $\lambda_p = 2\pi c \sqrt{\frac{\epsilon_o m}{n_o e^2}}$ is the plasma wavelength. A more

detailed treatment [14] shows that the correct scaling is $R_{sphere} = 2 \sqrt{\frac{n_b}{n_o}} \sigma_r$, where σ_r is the driving beam rms radius, that for a uniform cylindrical driving bunch gives $R_{sphere} = \sqrt{\frac{4eI}{\pi^3 mc^3 \epsilon_o}} \frac{\lambda_p}{2}$.

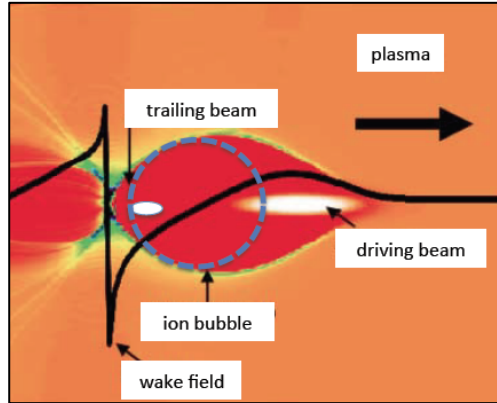


Fig. 9 – Schematic representation of the longitudinal wake field (black line) and ion distribution (red area) behind a driving laser or particle beam [11].

The field produced by the ions and experienced by a witness electron beam is purely electrostatic, being the ions at rest in the laboratory frame on the time scale of interest, and is simply given by:

$$(56) \quad E_r = \frac{en_o}{3\epsilon_o} r$$

i.e. it has a radial symmetry (other authors, see for example [12], consider a uniform charged cylindrical ion column producing a transverse field of the form $E_r = \frac{en_o}{2\epsilon_o} r$). The ion sphere is “virtually” moving along z with the speed β_d of the driving pulse due to the plasma electron collective oscillation, even if the source of the field remains at rest in the laboratory frame.

There are also magnetic fields produced by the plasma electron displacement but, as shown in ref. [15], the net effect on a relativistic beam is negligible.

The accelerating component of the field is linearly increasing from the moving sphere center $z_c = \beta_d ct$:

$$(57) \quad E_z(\xi) = \frac{en_o}{3\epsilon_o} \xi$$

where $\xi = z - z_c$, and has a maximum on the sphere edge at $\xi = \frac{\lambda_p}{2}$. The corresponding energy gained by a witness electron is given by $\gamma = \gamma_o + \alpha L_{acc}$ where L_{acc} is the accelerating length in the plasma and $\alpha(\xi) = \frac{eE_z(\xi)}{mc^2} = \frac{1}{3} \left(\frac{2\pi c}{\lambda_p} \right)^2 \xi$ is the normalized accelerating gradient.

The energy spread accumulated by a bunch of finite rms length σ_z is given by $\frac{\delta\gamma}{\gamma} = \frac{\delta\alpha L_{acc}}{\gamma_o + \alpha L_{acc}} \approx \frac{\delta\alpha}{\alpha} = \frac{\sigma_z}{\lambda_p}$, showing that ultra-short electron bunches are required to keep energy spread below 1%. In this simplified model beam loading effects are not considered as well as beam slippage with respect to the driving pulse.

The transverse (focusing) field:

$$(58) \quad E_x = \frac{en_o}{3\epsilon_o} x$$

at a distance x off the propagation axis is independent of ξ so that correlated emittance growth is not typically induced by the ion focusing field.

In fig. 10 are shown the plasma wavelength and the longitudinal and transverse fields experienced by a test particle located at $x=1 \mu\text{m}$ and $\xi = \frac{\lambda_p}{4}$ versus typical plasma densities, according to eqs. (54, 55).

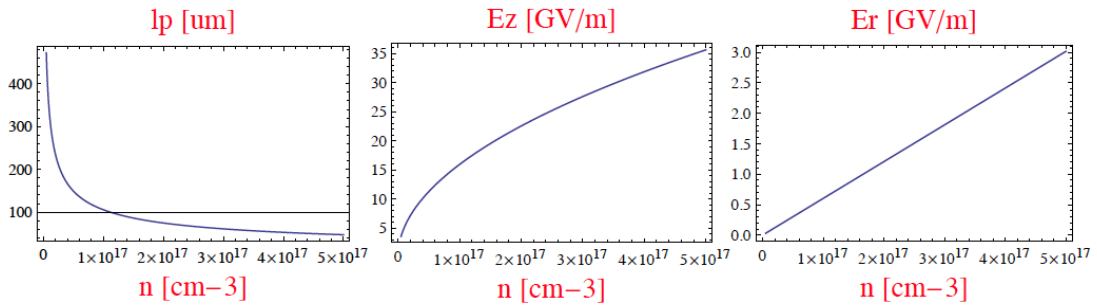


Fig. 10 - Plasma wavelength (left), longitudinal (center) and transverse (right) fields versus

typical plasma densities experienced by a test particle located at $x=1 \mu\text{m}$ and $\xi = \frac{\lambda_p}{4}$.

As discussed in the previous sections the transverse beam dynamics can be conveniently described by means of a proper envelope equation. To this end let us consider the single particle equation of motion:

$$(59) \quad x'' = \frac{F_x}{\beta c p} = \frac{e^2 n_o}{3 \epsilon_o \gamma m c^2} x = \frac{k_p^2}{3 \gamma} x$$

where $k_p = \sqrt{\frac{ne^2}{\epsilon_o mc^2}}$ is the plasma wave number. The moment of the force acting on the beam particles is given by

$$(60) \quad \langle x x'' \rangle = \frac{k_p^2}{3 \gamma} \langle x^2 \rangle = \frac{k_p}{3 \gamma} \sigma_x^2$$

Inserting in the envelope equation we obtain:

$$(61) \quad \sigma_x'' + \frac{\gamma'}{\gamma} \sigma_x' + \frac{k_p^2}{3 \gamma} \sigma_x = \frac{\epsilon_n^2}{\gamma^2 \sigma_x^3} + \frac{k_{sc}^o}{\gamma^3 \sigma_x}$$

An equilibrium solution of the previous equation has not yet been found, nevertheless some simplification is still possible and an approximated matching condition exists. As one can see there are two focusing terms, the adiabatic damping and the ion focusing, and two defocusing terms, the emittance pressure and the space charge effects. To compare the relative importance of the first two terms is more convenient to rewrite the previous equation with the new variable $\tilde{\sigma}_x = \sqrt{\gamma} \sigma_x$ leading to the equation:

$$(62) \quad \tilde{\sigma}_x'' + \left(\left(\frac{\gamma'}{2 \gamma} \right)^2 + \frac{k_p^2}{3 \gamma} \right) \tilde{\sigma}_x = \frac{\epsilon_n^2}{\tilde{\sigma}_x^3} + \frac{k_o^{sc}}{\gamma^2 \tilde{\sigma}_x}$$

The beam is space charge dominated, as already discussed in section 6, when:

$$(63) \quad \rho = \frac{k_o^{sc} \tilde{\sigma}_x^2}{\epsilon_n^2 \gamma^2} = \frac{k_o^{sc} \sigma_x^2}{\epsilon_n^2 \gamma} \gg 1$$

and ion focusing dominated when:

$$(64) \quad \eta = \frac{4 \gamma k_p^2}{3 \gamma'^2} \gg 1$$

With the typical beam parameters of a plasma accelerator: 1 kA peak current, 2 μm normalized emittance, injection energy $\gamma_o=300$ and spot size about 3 μm , we have $\rho < 1$ and

$\eta > 1$. It follows that the envelope equation can be well approximated by the following reduced expression:

$$(65) \quad \sigma_x'' + \frac{k_p^2}{3\gamma} \sigma_x = \frac{\epsilon_n^2}{\gamma^2 \sigma_x^3}$$

with $\gamma(z) = \gamma_o + \alpha z$. Looking for a particular solution in the form $\sigma_x = \gamma^{-1/4} \sigma_o$ we obtain:

$$(66) \quad \left(\frac{5}{16} \gamma'^2 + \frac{1}{3} \gamma k_p^2 \right) \sigma_o = \frac{\gamma \epsilon_n^2}{\sigma_o^3}$$

that for $\eta > 1$ has a simple solution $\sigma_o = \sqrt{\frac{\sqrt{3} \epsilon_n}{k_p}}$ giving the matching condition of the beam with the plasma:

$$(67) \quad \sigma_x = \gamma^{-1/4} \sigma_o = \sqrt[4]{\frac{3}{\gamma}} \sqrt{\frac{\epsilon_n}{k_p}}$$

In fig. 11 are shown the matched beam envelope given by eq. (67) with normalized emittance of 2 μm and injection energy $\gamma=300$ versus the plasma density. In the same figure is shown also the evolution of the beam envelope in a 10 cm long plasma with density 10^{16} cm^{-3} , corresponding to an accelerating field of 5 GV/m (extraction energy $\gamma=1300$) and focusing field of 60 MV/m.

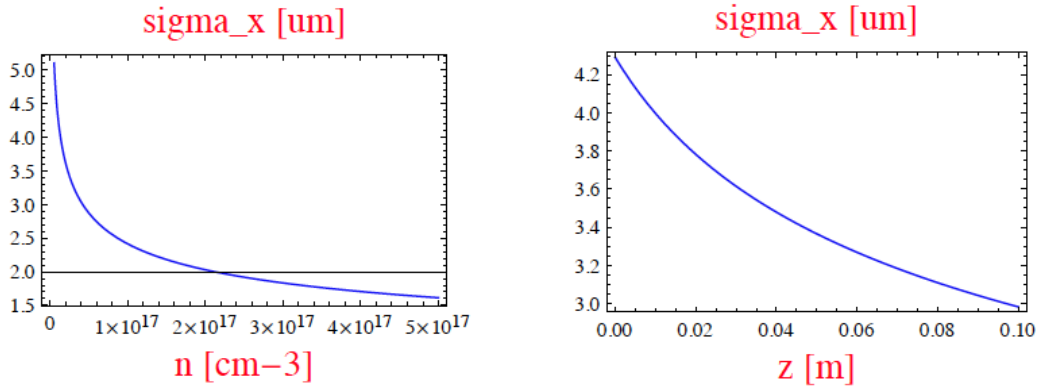


Fig. 11 - Matched beam envelope with normalized emittance of 2 μm and injection energy $\gamma=300$ versus the plasma density (right) and the evolution of the beam envelope in a 10 cm long plasma with density 10^{16} cm^{-3} , corresponding to an accelerating field of 5 GV/m and focusing field of 60 MV/m.

Notice that the beam experiences focusing as γ increases and the beam density increases leading to a significant perturbation of the plasma fields. A possible solution to overcome this effect is to taper the plasma density along the channel in order to achieve beam transport with constant envelope.

It is an interesting exercise to see the effect of a plasma density vanishing as $n(z) = \frac{\gamma_o}{\gamma(z)} n_o$, giving $k_p^2 = \frac{e^2 n_o}{\epsilon_o m c^2} \frac{\gamma_o}{\gamma} = \frac{\gamma_o}{\gamma} k_{o,p}^2$. In this case the envelope equation (61) without

space charge effects becomes:

$$(68) \quad \sigma_x'' + \frac{\gamma'}{\gamma} \sigma_x' + \frac{\gamma_o k_{o,p}^2}{3\gamma^2} \sigma_x = \frac{\epsilon_n^2}{\gamma^2 \sigma_x^3}$$

which admits a constant equilibrium solution:

$$(69) \quad \sigma_x = \sqrt[4]{\frac{3}{\gamma_o}} \sqrt{\frac{\epsilon_n}{k_{o,p}}}$$

Figure 12 shows the plasma density along the accelerating section and the resulting equilibrium beam envelope given by eq. (69) with the same beam parameters as of fig. 11

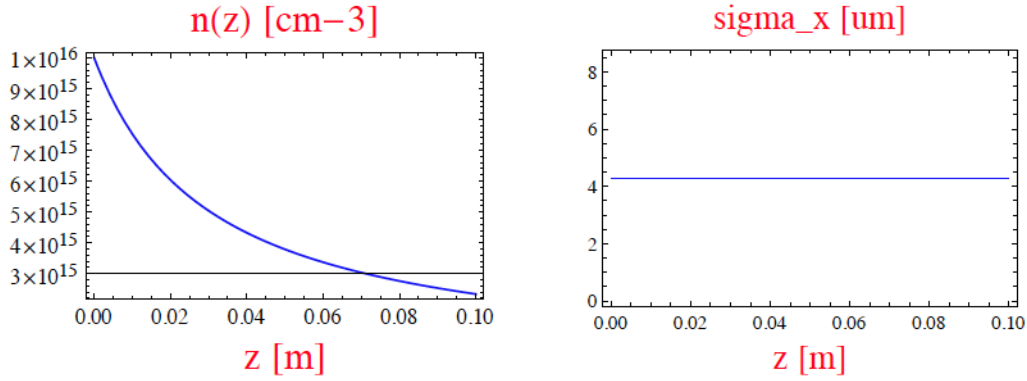


Fig. 12 - Plasma density along the accelerating section (left) and the resulting equilibrium beam envelope given by eq. (69) (right).

On the other hand before injection in the plasma accelerator, the beam has to be focused to the matching spot given by (67) to prevent envelope oscillations that may cause emittance growth and an enhancement of betatron radiation emission. It has been proposed [16] to shape the plasma density profile in order to gently capture the beam by means of the increasing ion focusing effect. For example by varying the plasma density as $n(z) = \frac{\gamma(z)}{\gamma_o} n_o$ at

the entrance of the plasma column, the envelope equation (61) can be written as

$$(70) \quad \sigma_x'' + \frac{k_{o,p}^2}{3\gamma_o} \sigma_x = \frac{\epsilon_n^2}{\gamma^2 \sigma_x^3}$$

with $k_p^2 = \frac{e^2 n_o}{\epsilon_o m c^2} \frac{\gamma}{\gamma_o} = \frac{\gamma}{\gamma_o} k_{o,p}^2$. This equation has a particular solution assuming that γ'' be negligible:

$$(71) \quad \sigma_x = \sqrt[4]{3\gamma_o} \sqrt{\frac{\epsilon_n}{\gamma k_{o,p}}}$$

showing that with a proper choice of the initial plasma density the beam envelope can be gently matched to the accelerating plasma channel.

For additional discussions about injection and extraction beam matching conditions see also

some recent paper: [22-25].

Acknowledgements

I wish to thank A. Cianchi, P. Muggli, J. B. Rosenzweig, A. R. Rossi and L. Serafini, for the many helpful discussions and suggestions.

References

- [1] T. Shintake, Proc. of the 22nd Particle Accelerator Conference, June 25-29, 2007, Albuquerque, NM (IEEE, New York, 2007), p. 89.
- [2] L. Serafini, J. B. Rosenzweig, PR E55 (1997) 7565
- [3] M. Reiser, “Theory and Design of Charged Particle Beams”, Wiley, New York, 1994
- [4] J. B. Rosenzweig, “Fundamentals of beam physics”, Oxford University Press, New York, 2003
- [5] T. Wangler, “Principles of RF linear accelerators”, Wiley, New York, 1998
- [6] S. Humphries, “Charged particle beams”, Wiley, New York, 2002
- [7] F. J. Sacherer, F. J., IEEE Trans. Nucl. Sci. NS-18, 1105 (1971).
- [8] M. Ferrario et al., Int. Journal of Modern Physics A, Vol 22, No. 23, 4214 (2007)
- [9] J. Buon, “Beam phase space and emittance”, in CERN 94-01
- [10] E. Esarey et al., Rev. of Modern Physics, V. 81, July–September 2009
- [11] C. Joshi and W. B. Mori, “The status and evolution of plasma wakefield particle accelerators”, Phil. Trans. R. Soc. A 2006 364, 577-585
- [12] J. B. Rosenzweig et al., Phys Rev A, V. 44, N. 10, 1991
- [13] P. Muggli and M. J. Hogan, “Review of high-energy plasma wakefield experiments”, C. R. Physique 10 (2009) 116–129
- [14] W. Lu et al., Phys. Plasmas 12 , 063101 (2005);
- [15] W. Lu et al., PRL 96, 165002 (2006)
- [16] P. Tomassini, private communication.
- [17] M. Migliorati et al., “Intrinsic normalized emittance growth in laser-driven electron accelerators”, Phys. Rev. ST Accel. Beams 16, 011302, 2013
- [18] M. Ferrario et al., Nucl. Instr. and Meth. in Phys. Res. B 309, (2013), 183–188
- [19] A. Cianchi et al., “Challenges in plasma and laser wakefield accelerated beams diagnostic”, Nucl. Instr. and Meth. in Phys. Res. A, V. 720, (2013), 153–156
- [20] Floettmann, “Some basic features of the beam emittance”, Phys. Rev. ST Accel. Beams 6, 034202 (2003).
- [21] N. Pichoff, Beam dynamics basics in RF linacs, proc. of CAS, CERN-2006-012.
- [22] R. Lehe et al., “Laser-plasma lens for laser-wakefield accelerators”, Phys. Rev. ST Accel. Beams 17, 121301 (2014).
- [23] T. Mehrling et al., “Transverse emittance growth in staged laser-wakefield acceleration”, Phys. Rev. ST Accel. Beams 15, 111303 (2012).
- [24] K. Floettmann, “Adiabatic matching section for plasma accelerated beams”, Phys. Rev. ST Accel. Beams 17, 054402 (2014)
- [25] I. Dornmair et al., “Emittance conservation by tailored focusing profiles in a plasma accelerator”, Phys. Rev. ST Accel. Beams 18, 041302 (2015)